13th Australasian Fluid Mechanics Conference
Monash University, Melbourne, Australia
13-18 December 1998

LABORATORY OBSERVATIONS OF INTERNAL WAVES

Bruce R. SUTHERLAND[1], Stuart B. DALZIEL[2], Graham O. HUGHES[3] and Paul F. LINDEN[2]

[1]Department of Mathematical Sciences
University of Alberta, Edmonton, Alberta T6G 2G1, CANADA

[2]Department of Applied Mathematics and Theoretical Physics
University of Cambridge, Cambridge CB3 9EW, U.K.

[3]Research School of Earth Sciences
The Australian National University, Canberra, A.C.T. 0200, AUSTRALIA

ABSTRACT

We present measurements of the internal wavefield produced in a stratified fluid by a simple vertically oscillating cylinder. A novel digital image-processing technique known as 'synthetic-schlieren' (Sutherland *et al.*, 1998) is described which allows the density and velocity fields to be determined by non-intrusive optical means. The synthetic-schlieren technique is used here to examine the effect of viscosity on the wavefield.

INTRODUCTION

In stratified environments such as the atmosphere and oceans, numerous mechanisms exist which locally disturb surfaces of constant density from their equilibrium position. As buoyancy forces seek to restore the local equilibrium, internal waves are commonly radiated away from the disturbed region. These waves transport both energy and momentum vertically, and as such, represent a very important process by which motion at different levels in a stratified flow can be coupled. However, much remains to be understood about the mechanisms responsible for the interaction and decay of internal waves.

In general, local disturbances apply a complex forcing to the stratified fluid over a range of timescales and spatial scales. An essential first step is to understand the simple but fundamentally important problem first considered by Mowbray & Rarity (1967), namely the wavefield produced by the monochromatic vertical oscillation of a cylinder in a stratified fluid. Mowbray & Rarity (1967) observed fluid motion to be confined to a 'St. Andrews Cross', consisting of four beams inclined at angles

$$\Theta = \pm \cos^{-1} \omega/N \qquad (1)$$

to the vertical, as predicted by linear theory (*e.g.* Lighthill, 1978). Here, ω (assumed $< N$) is the frequency of oscillation of the cylinder and N is the buoyancy frequency, defined for a Boussinesq stratified fluid as

$$N^2 = -\frac{g}{\rho_0}\frac{d\rho}{dz}, \qquad (2)$$

where g is the gravitational acceleration, ρ_0 is the mean fluid density and $d\rho/dz$ is the vertical density gradient.

Hurley & Keady (1997) presented approximate theoretical solutions for this problem, improving upon previous studies by considering the oscillation of a finite-sized cylinder in a viscous stratified fluid. In this study, we compare experimental measurements with the theoretical predictions of their model.

EXPERIMENTS

In all experiments, the tank shown in Figure 1 was linearly stratified with salt to a depth of 35 cm using the 'double-bucket' method. The density gradient was chosen such that the buoyancy frequency $N \approx 1\,\mathrm{s}^{-1}$. A cylinder of radius $R = 1.67$ cm was suspended from the supporting arm and immersed with its axis aligned horizontally and spanning the full width of the tank. The supporting arm was driven by an adjustable speed eccentric cam, forcing the cylinder to undergo sinusoidal vertical oscillations in time. The amplitude of cylinder oscillation A in the experiments described here was fixed at 0.32 cm.

The internal wavefield produced by the oscillating cylinder was visualised by using a camera (COHU 4910 Series High Performance Monochrome CCD) to view an image screen placed on the opposite side of the tank. In these experiments, the screen was translucent and backlit with a bank of fluorescent tubes so as to make the illumination as uniform as possible. The image itself consisted of black horizontal lines of thickness 0.2 cm on the screen and spaced at 0.4 cm intervals in the vertical. The camera was placed as far as practicable in front of the tank (3.5 m)

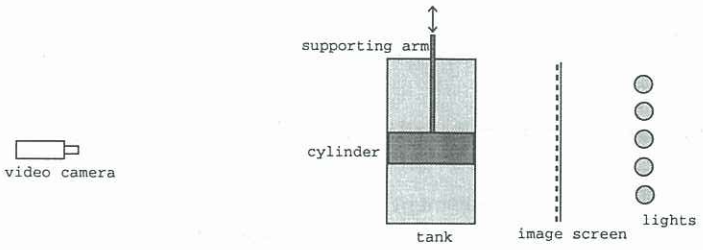

Figure 1: Experimental set-up for synthetic-schlieren visualisation (not to scale).

so as to minimise parallax error and, during an experiment, the images were recorded to video tape. With this arrangement, the field of view observed in the flow was 30 cm × 25 cm (horizontal × vertical).

During an experiment, the vertical motion of fluid perturbs the density field from equilibrium, inducing perturbations in the refractive index field. To an observer, the horizontal lines on the image screen will appear to be deflected vertically. For small perturbations, the apparent deflection of the lines Δz is proportional to the change in the density gradient field, *i.e.*,

$$\Delta z \approx \alpha \Delta N^2, \tag{3}$$

where α is a theoretically determined constant (Sutherland *et al.*, 1998) dependent upon the geometry of the experimental set-up and the properties of brine. The relation (3) can be integrated to find the density field throughout the flow and, by recording the time rate of change of ΔN^2, the velocity perturbation field can also be calculated. In these experiments, the video camera and the software package DigImage (Dalziel, 1992) are used to measure the apparent vertical deflection Δz at every point in the flow, and then to calculate the perturbation density and velocity fields. Measurements here, however, are presented in terms of the perturbation buoyancy frequency (proportional to the perturbation density gradient) field.

Although the optical principles described above correspond to those employed in traditional schlieren visualisation, the synthetic-schlieren technique used in this study has numerous advantages. First, large and expensive parabolic mirrors are not required. Hence, the field of view can be readily adjusted to suit the flow. Second, it is easier to make and adjust the sensitivity of quantitative measurements. Third, further information such as the velocity field can be readily calculated. As with traditional schlieren, however, synthetic-schlieren can only be used quantitatively for nominally two-dimensional flows.

RESULTS

In Figure 2, the internal wavefield produced in experiments by the vertical oscillation of the cylinder at four different frequencies ω is visualised in terms of the buoyancy frequency perturbation field ΔN^2. For each wavefield, only the beam radiating upwards and to the right is shown as the cylinder moves downwards past its equilibrium position. As the wavefield produced by a vertically oscillating cylinder is symmetric about the vertical and antisymmetric about the horizontal, the rest of the wavefield can be inferred in each case. The co-ordinate system has been rotated from the vertical by the angle Θ shown at the top left of each diagram and calculated using (1). Hence r is an along-beam co-ordinate and σ is the across-beam co-ordinate, with $\sigma = 0$ being aligned with the mean position of the cylinder centre. Note that an anisotropic scaling of the co-ordinate axes has been used, hence the elliptical appearance of the cylinder superposed on each diagram.

Several features are worthy of note.

The dispersion relation (1) obtained from linear theory is well supported in these experiments as the wave beams are closely aligned with the r axis in each case in Figure 2.

In regions where ΔN^2 is positive, the surfaces of constant density have been compressed vertically and the local buoyancy frequency is greater than the ambient value given by (2). Hence, the largest values of ΔN^2 correspond to regions where the internal wave amplitude is also largest. For each frequency of cylinder oscillation in Figure 2, it is apparent that the wave amplitude is attenuated with radial distance from the cylinder. As the fluid response forced by the cylinder is almost entirely in the along-beam direction, this attenuation is primarily due to the action of viscous forces on velocity gradients in the across-beam (σ) direction. Further, it can be seen that viscous attenuation modifies the structure of the wave beam with radial distance from the cylinder. At small r, the maximum internal wave amplitude is observed to be toward the edges of the beam at $\sigma \approx \pm R$, and the displacement of fluid elements from their equilibrium position has a double-peaked (bimodal) distribution. However, at larger r, the internal wave amplitude tends to have a maximum at the centre of the wave beam. Hence the fluid displacement is characterised by a single-peaked (unimodal) structure, which in these experiments was observed to de-

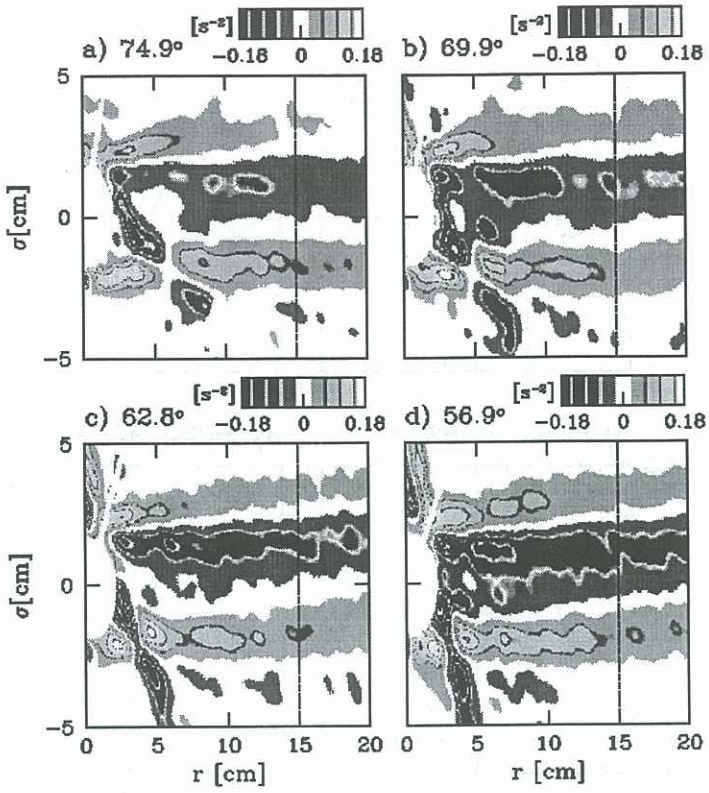

Figure 2: The internal wavefield generated by a cylinder oscillating vertically at frequencies (a) $\omega = 0.26\,\mathrm{s}^{-1}$, (b) $\omega = 0.34\,\mathrm{s}^{-1}$, (c) $\omega = 0.46\,\mathrm{s}^{-1}$ and (d) $\omega = 0.55\,\mathrm{s}^{-1}$. Visualisation of the wavefield is in terms of ΔN^2 with the grey scale ranging from $-0.18\,\mathrm{s}^{-1}$ to $0.18\,\mathrm{s}^{-1}$.

velop at a distance $r/R \sim 8$. To date, theoretical studies have offered little insight into this transitional behaviour, and this is currently the subject of further investigation.

The structure of the wavefield is very similar at each forcing frequency shown in Figure 2. The width of the beam is similar in each case and, as observed in previous studies (*e.g.* Thomas & Stevenson, 1972), increases gradually with distance r. Viscous attenuation of the fluid motion can again be used to explain this observation. The transverse structure of the along-beam fluid response at a given position r can be considered to be the superposition of numerous modes. Viscosity will preferentially attenuate those modes with the most rapid variation in the σ direction. Hence modes which are characterized by longer lengthscales in the σ direction will predominate as r increases, tending to increase the beam width.

As the forcing frequency decreases, it is apparent from Figure 2 that the amplitude of the fluid response also decreases. The reason for this is that the energy input from the source is radiated more efficiently along the wave beams when the forcing is at a lower frequency. Therefore, the energy density available to drive fluid motion in the wave beam is also reduced, leading to internal waves of smaller amplitude. This can be understood qualitatively by considering the group velocity c_g at which energy is transported in the along-beam direction. Linear theory gives

$$c_g = \frac{N}{k_\sigma} \sin\Theta, \tag{4}$$

where k_σ is a wavenumber characterising the wavefield structure in the across-beam direction. As the across-beam structure, and therefore k_σ, is similar for the four cases shown in Figure 2, the group velocity c_g can be seen from (1) and (4) to increase as the forcing frequency ω decreases.

In Figure 3, some experimental measurements are compared with the approximate theoretical solution of Hurley & Keady (1997) for an internal wavefield attenuated by viscosity. The comparison is made along the dotted sections perpendicular to the wave beam shown in Figure 2, at $r/R = 9$. The perturbation density gradient values in Figure 3 have been normalised by the amplitude of cylinder oscillation $A = 0.32\,\mathrm{cm}$. Although the theoretical solution (shown as a solid line) agrees well with experimental measurements, there are some systematic discrepancies. Estimates of the beam width based on the distance between maxima and minima or between zeroes in the observed wave amplitude distribution are consis-

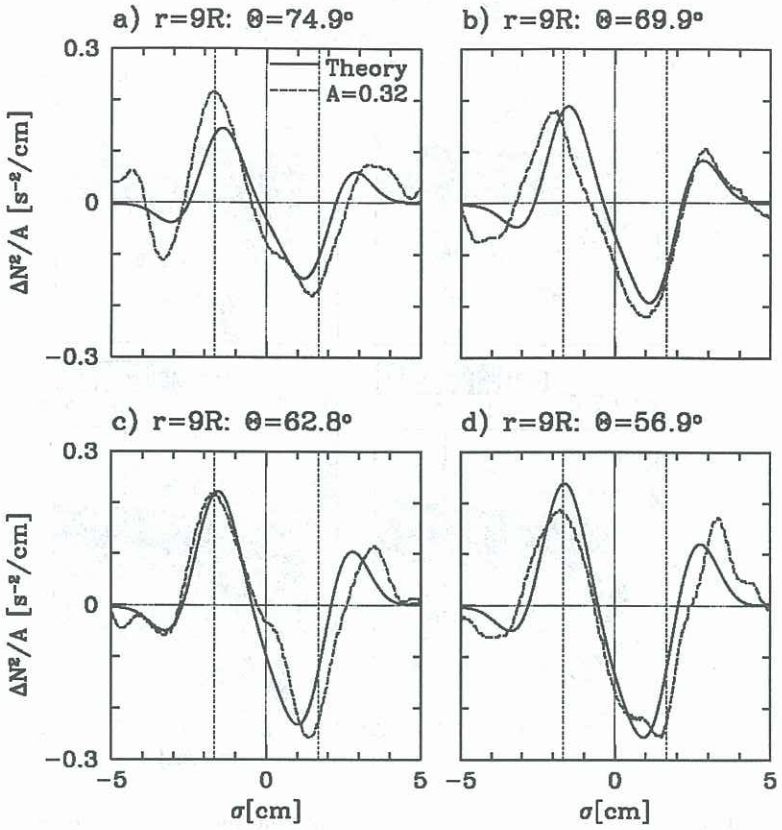

Figure 3: Comparison of experimental measurements (dotted line) and theoretical predictions (solid line) for the wave beam structure at $r/R = 9$ generated by a cylinder oscillating vertically at frequencies (a) $\omega = 0.26\,\mathrm{s}^{-1}$, (b) $\omega = 0.34\,\mathrm{s}^{-1}$, (c) $\omega = 0.46\,\mathrm{s}^{-1}$ and (d) $\omega = 0.55\,\mathrm{s}^{-1}$.

tently larger than theory would suggest. This is due to the existence of a laminar viscous boundary layer surrounding the oscillating cylinder, which effectively increases the size of the source — in this instance by approximately 15%. At lower forcing frequencies, the theoretical solution over-predicts the measured internal wave amplitude, while at higher frequencies the fluid response is under-predicted. The reason for this is not understood at present.

CONCLUSIONS

We have revisited the problem of internal wave generation by a vertically oscillating cylinder in a stratified fluid. Using a new visualisation technique we have been able to examine the structure of the internal wavefield and to compare amplitude measurements with recent theoretical solutions. This comparison has suggested areas in which the theory needs to be improved, and is also the motivation for work currently underway to better understand the transport of energy by internal waves radiated from different types of source, together with the role played by viscous dissipation.

REFERENCES

DALZIEL, S.B., "Decay of rotating turbulence: Some particle tracking experiments.", *Appl. Sci. Res.*, **5**, 217–244, 1992.

HURLEY, D.G. & KEADY, G., "The generation of internal waves by vibrating cylinders, Part 2: Approximate viscous solution for a circular cylinder.", *J. Fluid Mech.*, **351**, 119–138, 1997.

LIGHTHILL, M.J., *Waves in Fluids*, Cambridge University Press, Cambridge, England, 1978.

MOWBRAY, D.E. & RARITY, B.S.H., "A theoretical and experimental investigation of the phase configuration of internal waves of small amplitude in a density stratified liquid.", *J. Fluid Mech.*, **28**, 1–16, 1967.

SUTHERLAND, B.R., DALZIEL, S.B., HUGHES, G.O. & LINDEN, P.F., "Visualisation and measurement of internal waves by 'synthetic schlieren'. Part 1: Vertically oscillating cylinder.", *J. Fluid Mech.*, submitted, 1998.

THOMAS, N.H. & STEVENSON, T.N., "A similarity solution for viscous internal waves.", *J. Fluid Mech.*, **54**, 495–506, 1972.